Active Antenna Selection in Multiuser MIMO Communications

Mirette Sadek, *Student Member, IEEE*, Alireza Tarighat, *Member, IEEE*, and Ali H. Sayed, *Fellow, IEEE*

***Abstract*—The paper develops a dynamic antenna scheduling strategy for downlink MIMO communications, where a subset of the receive antennas at certain users is selectively disabled. The proposed method improves the signal-to-leakage-plus-noise (SLNR) ratio performance of the system and it relaxes the condition on the number of transmit-receive antennas in comparison to traditional zero-forcing and time-scheduling strategies. The largest value that the SLNR can achieve is shown to be equal to the maximum eigenvalue of a certain random matrix combination, and the probability distribution of this eigenvalue is characterized in terms of a Whittaker function. The result shows that increasing the number of antennas at some users can degrade the SLNR performance at other users. This fact is used to propose an antenna scheduling scheme that leads to improvement in terms of SINR outage probabilities.**

***Index Terms*—Antenna selection, beamforming, eigenvalue distribution, leakage, multiple-input multiple-output (MIMO) systems, multiuser communications.**

I. Introduction

MULTIPLE-INPUT MULTIPLE-OUTPUT (MIMO) schemes can provide a substantial gain in network downlink throughput by allowing multiple users to communicate in the same frequency and time slots. The downlink transmitter design problem has been studied under different conditions. For instance, in [1] the problem was studied under the condition of a single receive antenna per user. However, the multiplicity of users and antennas causes cochannel interference (CCI) among users. Several works in the literature have proposed schemes for perfectly canceling the CCI for each user. Some schemes have suggested iterative algorithms to solve the multiuser optimization problem and cancel the CCI [2], [3]. Other schemes have provided closed form solutions. Most notable among these schemes are the so-called zero forcing (ZF) solutions [4]–[7]. These ZF designs tend to ignore the additive noise component at the receivers when designing the beamforming vectors at the transmitter. Receivers using the values of these beamforming vectors for decoding will suffer from noise enhancement. In addition, ZF designs impose a restriction on the system configuration in terms of the number of antennas. Roughly, ZF methods require the number of transmit antennas at the base station to be larger than the combined sum of all receive antennas by all users. This condition is necessary in order to provide enough degrees of freedom for the zero-forcing solution to be able to force the CCI to zero at each user. The condition can be impractical and one way to alleviate it is to resort to time-scheduling [8]. In this scheme, a subset of the users is allowed to communicate at each time slot such that the total number of receive antennas for active users at any time instant satisfies the required dimension condition [9]. Such scheduling schemes basically shut down some of the users in the network at any given time so that the remaining users can establish a connection.

Several other antenna selection schemes have been previously studied in the literature, but mainly for single-user MIMO communications by using antenna selection criteria that range from minimizing the symbol error rate, to maximizing the channel capacity, or increasing the diversity gain [10]. Antenna selection has also been studied in MIMO systems employing orthogonal space time block coding (OSTBC) [11]–[13]. In this paper, we propose an alternative criterion for active antenna selection in *multiuser* (as opposed to single-user) MIMO systems. Specifically, the contribution of the paper is twofold. Using the concept of *leakage* introduced in [14], [15] (and reviewed in Section II), we define a performance metric in terms of the so-called signal-to-leakage-plus-noise (SLNR) ratio. The beamforming vectors at the transmitter are designed such that the SLNR metric is maximized for each user. The solution is suboptimal in terms of the output SINR metric but provides a closed form expression for the beamforming vectors that are otherwise solved for iteratively [3]. We show that the largest value that the SLNR ratio can achieve is equal to the maximum eigenvalue of a certain random matrix combination (which is defined in terms of the channel matrices). We subsequently study the probability density function of this maximum eigenvalue and characterize it in terms of a so-called Whittaker function. The resulting analysis establishes that increasing the number of receive antennas at some other users degrades the SLNR at the desired user. This result is specific to the SLNR criterion. The result is exploited to suggest a multiuser spatial multiplexing scheme that reduces the number of active antennas for users not meeting an SINR threshold for any antenna configuration and activates a subset of the receive antennas for every user that meets the target SINR.

There are two main scenarios where the proposed selection scheme can be useful. The first scenario is when a user is above its SINR threshold and has a large number of antennas. Decreasing the number of active receive antennas for this user would still keep it above its SINR threshold and would help the other users achieve their SINR threshold with a higher probability. The other scenario is when a user is below its SINR

Manuscript received July 22, 2005; revised May 23, 2006. This work was supported in part by the NSF by Grants CCF-0208573 and ECS-0401188. The associate editor coordinating the review of this paper and approving it for publication was Dr. Luc Vandendorpe.

The authors are with the Department of Electrical Engineering, University of California, Los Angeles, CA 90095 USA (e-mail: mirette@ee.ucla.edu; tarighat@ee.ucla.edu; sayed@ee.ucla.edu).

Color versions of figures available online at http://ieeexplore.ieee.org.
Digital Object Identifier 10.1109/TSP.2006.888893

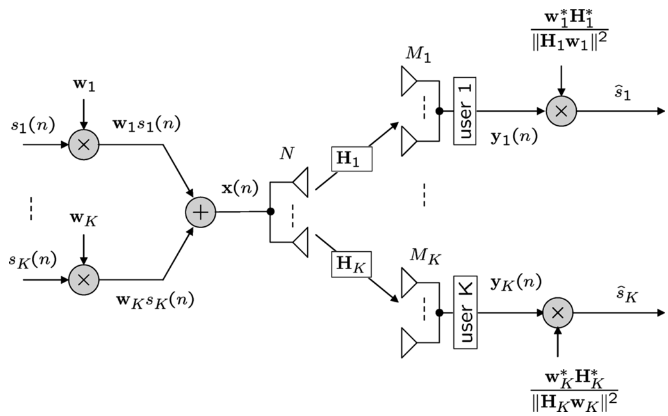

Fig. 1. Block diagram of the multiuser beamforming system.

threshold and decreasing the number of its active antennas would help other users achieve a higher SINR and possibly meet their SINR threshold.

This paper is organized as follows. In Section II the system model is introduced. Section III provides an analysis for the probability density function of the SLNR as a function of system parameters. The active antenna selection scheme is described in Section IV. Simulation results for different scenarios are shown in Sections V and VI concludes the paper.

II. System Model

Consider a downlink multiuser environment with a base station communicating with K users. The base station employs N transmit antennas and each user could be equipped with multiple antennas as well. Let M_i denote the number of receive antennas at the ith user. A block diagram of the system is shown in Fig. 1, where $s_i(n)$ denotes the transmitted data intended for user i at time n. The scalar data $s_i(n)$ is multiplied by an $N \times 1$ beamforming vector $\mathbf{w}_i$ before being transmitted over the channel. In this way, the overall $N \times 1$ transmitted vector at time n is given by

$$\mathbf{x}(n) = \sum_{k=1}^{K} \mathbf{w}_k s_k(n) (N \times 1). \tag{1}$$

The data $s_i(n)$ and the beamforming coefficients $\mathbf{w}_i$ are assumed to be normalized as follows:

$$\mathsf{E}|s_k(n)|^2 = 1, \quad \|\mathbf{w}_k\|^2 = 1$$

for $k = \{1, \ldots, K\}$.

The $N \times 1$ vector $\mathbf{x}(n)$ is then broadcast over the channel. Assuming a narrow-band (single-path) channel, the received vector of size $M_i \times 1$ at the ith user at time n is given by

$$\mathbf{y}_i(n) = \mathbf{H}_i \sum_{k=1}^{K} \mathbf{w}_k s_k(n) + \mathbf{v}_i(n) (M_i \times 1) \tag{2}$$

where the entries of the $M_i \times N$ channel matrix $\mathbf{H}_i$ are denoted by

$$\mathbf{H}_i = \begin{bmatrix} h_i^{(1,1)} & \cdots & h_i^{(1,N)} \\ \vdots & \ddots & \vdots \\ h_i^{(M_i,1)} & \cdots & h_i^{(M_i,N)} \end{bmatrix} \quad (M_i \times N) \tag{3}$$

with $h_i^{(k,l)}$ representing the channel coefficient from the lth antenna at the base station to the kth receiver antenna at user i. The elements of $\mathbf{H}_i$ are complex Gaussian variables with zero-mean and unit-variance. Furthermore, the additive noise $\mathbf{v}_i(n)$ is spatially and temporarily white with mean zero and variance

$$\mathsf{E}\mathbf{v}_i\mathbf{v}_i^* = \sigma_i^2 \mathbf{I}_{M_i}$$

where $\mathbf{I}_{M_i}$ is the $M_i \times M_i$ identity matrix. It is assumed that each channel matrix $\mathbf{H}_i$ is available at the base station and at the corresponding user, but is not required to be known by the other users. Dropping the time index n for notational simplicity we rewrite (2) as

$$\mathbf{y}_i = \mathbf{H}_i \mathbf{w}_i s_i + \sum_{k=1, k\neq i}^{K} \mathbf{H}_i \mathbf{w}_k s_k + \mathbf{v}_i \quad (M_i \times 1) \tag{4}$$

where the second term is the CCI caused by the multiuser nature of the system.

The signal-to-interference-plus-noise ratio (SINR) at the *input* of the receiver is given by

$$\text{SINR}_i = \frac{\|\mathbf{H}_i \mathbf{w}_i\|^2}{M_i \sigma_i^2 + \sum_{k=1, k\neq i}^{K} \|\mathbf{H}_i \mathbf{w}_k\|^2}. \tag{5}$$

Using the SINR expression in (5) as an optimization criterion for determining the beamforming vectors $\{\mathbf{w}_i\}_{i=1}^{K}$ generally results in a challenging optimization problem with K coupled variables $\{\mathbf{w}_i\}$ [16], [17].

One way to avoid solving the coupled problem is to cancel the CCI completely by using zero-forcing (ZF) schemes. For example in [4] and [7], the criterion for choosing the beamforming vectors $\mathbf{w}_i$, $i = \{1, \ldots, K\}$, has been to enforce

$$\mathbf{H}_i \mathbf{w}_k = \mathbf{0} \quad \text{for all } i, k = \{1, \ldots, K\}, i \neq k. \tag{6}$$

This ZF scheme requires the following condition on the number of antennas

$$N > \max_i \left\{ \sum_{k=1, k\neq i}^{K} M_k \right\}. \tag{7}$$

That is, the number of transmit antennas essentially needs to be as large as the number of all receive antennas combined. Thus the scheme (6) requires an increase in the number of base station antennas as the number of users or the number of receive antennas per user increase. Also, the ZF solution can lead to a small signal-to-noise ratio since it ignores the noise power in finding $\mathbf{w}_i$. For these reasons, we have formulated in [14] and [15] an alternative criterion that relaxes the requirement (7) and that takes the noise contribution into account when choosing $\mathbf{w}_i$. The criterion is based on defining a so-called *signal-to-leakage-plus-noise ratio* (SLNR). It leads to a closed form characterization of the optimal $\{\mathbf{w}_i\}$ in terms of generalized eigenvalue problems. Moreover, the scheme does not require the dimensionality condition (7).

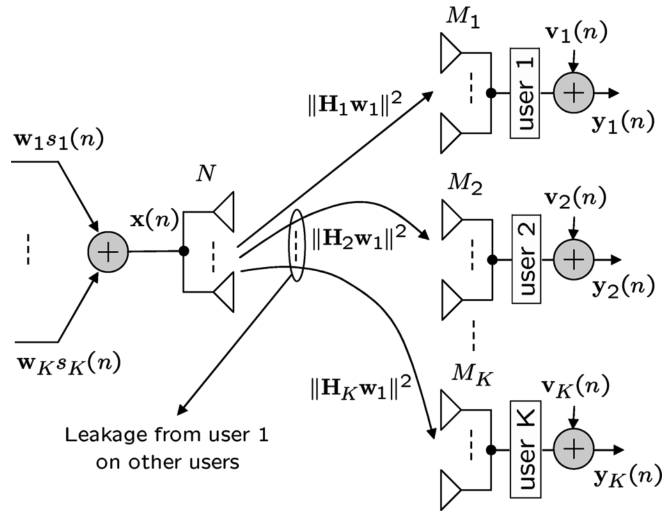

Fig. 2. A block diagram depicting the leakage from user 1 on other users.

Considering (4), we note that the power of the desired signal component for user i is given by $\|\mathbf{H}_i\mathbf{w}_i\|^2$. At the same time, the power of the interference that is caused by user i on the signal received by some other user k is given by $\|\mathbf{H}_k\mathbf{w}_i\|^2$. We, thus, defined in [14] and [15] a quantity, called *leakage* for user i, as the total power leaked from this user to all other users—see Fig. 2

$$\sum_{k=1,k\neq i}^{K} \|\mathbf{H}_k\mathbf{w}_i\|^2.$$

For each user i, we would like its signal power, $\|\mathbf{H}_i\mathbf{w}_i\|^2$, to be large compared to the noise power at its receiver (i.e., $M_i\sigma_i^2$). We would also like $\|\mathbf{H}_i\mathbf{w}_i\|^2$ to be large compared to the power leaked from user i to all other users, i.e., $\sum_{k=1,k\neq i}^{K}\|\mathbf{H}_k\mathbf{w}_i\|^2$. These considerations motivated us to introduce a figure of merit in terms of so-called signal-to-leakage-noise ratio (SLNR) defined as [14], [15]

$$\mathrm{SLNR}_i = \frac{\|\mathbf{H}_i\mathbf{w}_i\|^2}{M_i\sigma_i^2 + \sum_{k=1,k\neq i}^{K}\|\mathbf{H}_k\mathbf{w}_i\|^2}. \tag{8}$$

Thus note that in interference limited scenarios, the criterion reduces to maximizing the ratio $\|\mathbf{H}_i\mathbf{w}_i\|^2/\sum_{k=1,k\neq i}^{K}\|\mathbf{H}_k\mathbf{w}_i\|^2$. Maximizing this quantity for all users in the system *simultaneously* will improve the SIR for every user. On the other hand, in noise limited scenarios, the optimization criterion reduces to maximizing the SNR $\|\mathbf{H}_i\mathbf{w}_i\|^2/M_i\sigma_i^2$.

Using this concept of leakage, we have formulated in [14] the following decoupled optimization problem:

$$\mathbf{w}_i^o = \arg\max_{\mathbf{w}_i\in\mathbb{C}^{N\times 1}} \underbrace{\frac{\|\mathbf{H}_i\mathbf{w}_i\|^2}{M_i\sigma_i^2 + \sum_{k=1,k\neq i}^{K}\|\mathbf{H}_k\mathbf{w}_i\|^2}}_{\text{SLNR for user}} \; i \tag{9}$$

subject to $\|\mathbf{w}_i\|^2 = 1, i = \{1,\ldots,K\}$. In this cost function, the numerator measures the power of the signal intended for user i, while the denominator measures the power that leaks from user i to all other users in addition to the noise power at the receiver of the ith user—see Fig 2.

The vector $\mathbf{w}_i^o$ that solves (9) is not optimal relative to the SINR criterion (5), which is the criterion that is ultimately used to evaluate the system performance. As aforementioned, optimizing (5) over $\mathbf{w}_i$ is challenging and we are therefore proposing the alternative SLNR criterion (9). While our solution is only optimal relative to the SLNR; it allows us to achieve a closed-form solution with a good performance—see Fig. 8.

Problem (9) can be rewritten as

$$\mathbf{w}_i^o = \arg\max_{\mathbf{w}_i\in\mathbb{C}^{N\times 1}} \frac{\mathbf{w}_i^*\mathbf{H}_i^*\mathbf{H}_i\mathbf{w}_i}{\mathbf{w}_i^*(M_i\sigma_i^2\mathbf{I} + \tilde{\mathbf{H}}_i^*\tilde{\mathbf{H}}_i)\mathbf{w}_i} \tag{10}$$

subject to $\|\mathbf{w}_i\|^2 = 1$where

$$\tilde{\mathbf{H}}_i = [\mathbf{H}_1\mathbf{H}_{i-1}\mathbf{H}_{i+1}\cdots\mathbf{H}_K]^T \quad \left(\sum_{\substack{j=1\\ j\neq i}}^{K} M_j \times N\right) \tag{11}$$

is an extended channel matrix that excludes $\mathbf{H}_i$ only. Here, $[\cdot]^T$ denotes the transpose operation. To solve (9) we note that, in view of the Rayleigh-Ritz quotient result [18], the optimum beamforming vector $\mathbf{w}_i^o$ is given by

$$\mathbf{w}_i^o \propto \max.\text{generalized eigenvector} \times \left(\mathbf{H}_i^*\mathbf{H}_i, M_i\sigma_i^2\mathbf{I} + \tilde{\mathbf{H}}_i^*\tilde{\mathbf{H}}_i\right) \tag{12}$$

in terms of the eigenvector corresponding to the largest generalized eigenvalue of the matrices $\mathbf{H}_i^*\mathbf{H}_i$ and $M_i\sigma_i^2\mathbf{I} + \tilde{\mathbf{H}}_i^*\tilde{\mathbf{H}}_i$.

Since $(M_i\sigma_i^2\mathbf{I} + \tilde{\mathbf{H}}_i^*\tilde{\mathbf{H}}_i)$ is invertible, the generalized eigenvalue problem (12) actually reduces to a standard eigenvalue problem, namely

$$\mathbf{w}_i^o \propto \max\ \text{eigenvector}\left(\left(M_i\sigma_i^2\mathbf{I} + \tilde{\mathbf{H}}_i^*\tilde{\mathbf{H}}_i\right)^{-1}\mathbf{H}_i^*\mathbf{H}_i\right) \tag{13}$$

in terms of the eigenvector that corresponds to the maximum eigenvalue of $(M_i\sigma_i^2\mathbf{I} + \tilde{\mathbf{H}}_i^*\tilde{\mathbf{H}}_i)^{-1}\mathbf{H}_i^*\mathbf{H}_i$, say $\lambda_{\max}$. The proportionality constant is chosen such that the norm of $\mathbf{w}_i^o$ is scaled to $\|\mathbf{w}_i^o\|^2 = 1$. Choosing $\mathbf{w}_i^o$ according to (13) results in a maximum SLNR given by

$$\mathrm{SLNR} = \lambda_{\max}. \tag{14}$$

Fig. 3 from [14] and [15] is a plot of the SINR outage curves using three different schemes, namely, the proposed SLNR-based scheme (13) (using the full number of receive antennas), the zero-forcing (ZF) scheme (6) and a single-user beamforming scheme which ignores the CCI when selecting the beamforming vectors given by [19]

$$\mathbf{w}_i^o \propto \max\ \text{eigenvector}(\mathbf{H}_i^*\mathbf{H}_i). \tag{15}$$

These three schemes are compared to a hypothetical interference-free scenario, which is added in the plot only for comparison purposes. In the interference-free scenario, the beamforming vectors $\{\mathbf{w}_i\}$ are designed according to (15) and the

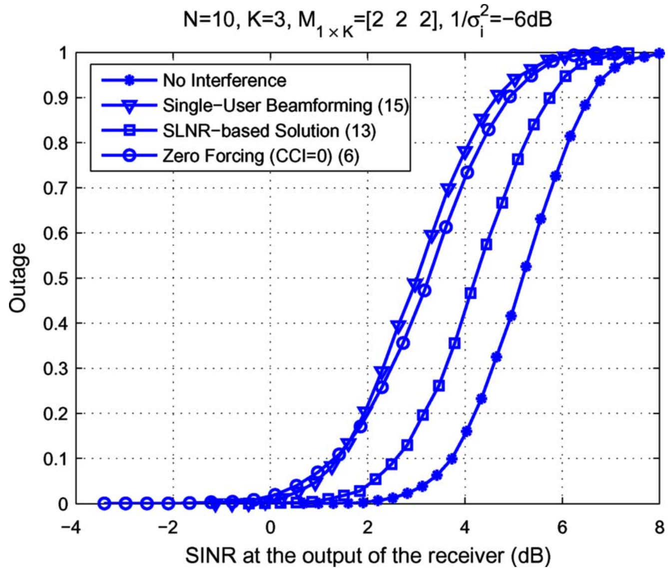

Fig. 3. SINR outage probability for one user comparing three different schemes with the ideal interference-free case.

simulations assume no CCI at the receiver, i.e., it is a scenario where we assume the K-user system is decoupled into K single-user systems that do not interfere with each other. In the simulations, a matched filter was used at the receiver for all of these schemes. Using a matched filter at the receiver, the decoded symbol $\hat{s}_i$ at user i is given by

$$\hat{s}_i = \tilde{\mathbf{w}}_i^* \mathbf{y}_i \tag{16}$$

where

$$\tilde{\mathbf{w}}_i^* = \frac{\mathbf{w}_i^* \mathbf{H}_i^*}{\|\mathbf{H}_i \mathbf{w}_i\|}.$$

The figure shows that the SLNR-based scheme outperforms the ZF scheme.

One of the purposes of this paper is to examine how the SLNR (14) can be further improved. In the next section, we examine how $\lambda_{\max}$ varies with the system parameters $\{N, K, M_i\}$. The ensuing analysis will suggest a dynamic way for adjusting the number of receive antennas M_i for each user in order to enhance the system performance.

A key step towards quantifying the dependence of $\lambda_{\max}$ on $\{N, K, M_i\}$ is to derive an expression for its probability density function (pdf). To do so, we shall rely on results from the theory of random matrices [20]–[23] and on the approach of [24].

III. Maximum Eigenvalue Distribution

Thus consider first the following generic problem statement.

Problem Statement: Given an $s \times m$ matrix $\mathbf{\Phi}$ and a $t \times m$ matrix $\tilde{\mathbf{\Phi}}$, both with complex i.i.d. zero-mean unit-variance Gaussian elements, we would like to characterize the probability density function (pdf) of the maximum eigenvalue $\lambda_{\max}$ of the matrix combination $(\sigma^2 \mathbf{I} + \tilde{\mathbf{\Phi}}^* \tilde{\mathbf{\Phi}})^{-1} \mathbf{\Phi}^* \mathbf{\Phi}$, where $\sigma^2 > 0$. The matrices $\mathbf{\Phi}$ and $\tilde{\mathbf{\Phi}}$ are assumed to be statistically independent.

Note that the expression

$$\left(M_i \sigma_i^2 \mathbf{I} + \tilde{\mathbf{H}}_i^* \tilde{\mathbf{H}}_i\right)^{-1} \mathbf{H}_i^* \mathbf{H}_i \tag{17}$$

is covered by this formulation by choosing

$$\begin{aligned} \mathbf{\Phi} = \mathbf{H}_i, \quad \tilde{\mathbf{\Phi}} = \tilde{\mathbf{H}}_i, \quad s = M_i, \quad m = N \\ t = \sum_{\substack{j=1 \\ j \neq i}}^{K} M_j, \quad \sigma^2 = M_i \sigma_i^2. \end{aligned} \tag{18}$$

In this paper, we focus on the case where $\mathbf{\Phi}$ and $\tilde{\mathbf{\Phi}}$ are tall matrices, i.e., $s > m$ and $t > m$. This condition translates to the case where the number of transmit antennas is less than the number of receive antennas, i.e.,

$$N < \min_i \{M_i\} \quad \text{and} \quad N < \min_i \left\{ \sum_{\substack{j=1 \\ j \neq i}}^{K} M_j \right\}. \tag{19}$$

There have been several interesting works in the literature on the joint pdf of the eigenvalues of some random matrix combinations. These earlier results do not apply to a combination of the general form $(\sigma^2 \mathbf{I} + \tilde{\mathbf{\Phi}}^* \tilde{\mathbf{\Phi}})^{-1} \mathbf{\Phi}^* \mathbf{\Phi}$, which includes a regularization parameter $\sigma^2 > 0$. Let $\mathbf{A}$ and $\mathbf{B}$ denote the $m \times m$ Hermitian matrices defined by $\mathbf{A} = \mathbf{\Phi}^* \mathbf{\Phi}$ and $\mathbf{B} = \tilde{\mathbf{\Phi}} \tilde{\mathbf{\Phi}}$. Earlier studies have examined the distribution of the eigenvalues of matrix combinations of the form $\mathbf{B}^{-1}\mathbf{A}$ [24] and $(\mathbf{B} + \mathbf{A})^{-1}\mathbf{A}$ [25]. In the sequel, we show how to extend the argument of [25] to treat the form $(\sigma^2 \mathbf{I} + \mathbf{B})^{-1}\mathbf{A}$. The ensuing analysis will require that we resort to the so-called Whittaker function [23].

To proceed, it is known that $\mathbf{A}$ has a complex Wishart distribution with m degrees of freedom, denoted by $\mathbf{A} \sim \mathbf{W}_m(0, \mathbf{I}_m)$. Moreover, the joint probability density function (pdf) of the elements of $\mathbf{A}$ is given by [23], [24]

$$f(\mathbf{A}) = \frac{1}{\tilde{\Gamma}_m(s)} e^{-\mathsf{Tr}\mathbf{A}} \cdot |\mathbf{A}|^{s-m} \tag{20}$$

where $\tilde{\Gamma}_m(s)$ is the complex multivariate Gamma function that is defined in terms of the ordinary Gamma function $\Gamma(s)$ as follows [24]:

$$\begin{aligned} \tilde{\Gamma}_m(s) &= \pi^{\frac{1}{2}m(m-1)} \prod_{i=1}^{m} \Gamma(s - i + 1) \\ \Gamma(s) &= \int_0^\infty t^{s-1} e^{-t}\, dt \end{aligned} \tag{21}$$

In (20), the notation $\mathsf{Tr}(.)$ denotes the trace of its argument and the notation $|\cdot|$ denotes the *absolute value* of the determinant of its argument. Similarly, $\mathbf{B}$ has a Wishart distribution with m degrees of freedom, denoted by $\mathbf{B} \sim \mathbf{W}_m(0, \mathbf{I}_m)$. The joint pdf of the elements of $\mathbf{B}$ is likewise given by

$$f(\mathbf{B}) = \frac{1}{\tilde{\Gamma}_m(t)} e^{-\mathsf{Tr}\mathbf{B}} \cdot |\mathbf{B}|^{t-m}. \tag{22}$$

Since $\mathbf{\Phi}$ and $\tilde{\mathbf{\Phi}}$ are statistically independent, then $\mathbf{A}$ and $\mathbf{B}$ are also independent. It follows that the joint pdf of the elements of $\mathbf{A}$ and $\mathbf{B}$ is given by

$$f(\mathbf{A},\mathbf{B}) = \frac{1}{\tilde{\Gamma}_m(s)\tilde{\Gamma}_m(t)} e^{-\mathsf{Tr}(\mathbf{A}+\mathbf{B})} \cdot |\mathbf{A}|^{s-m} \cdot |\mathbf{B}|^{t-m}. \tag{23}$$

Our objective is to derive the joint pdf of the eigenvalues of $(\sigma^2\mathbf{I}+\mathbf{B})^{-1}\mathbf{A}$. Introduce the Hermitian positive definite matrix $\mathbf{G} = \sigma^2\mathbf{I}+\mathbf{B}$ and let $\mathbf{G}^{(1/2)}$ denote its Hermitian square root, i.e., $\mathbf{G} = \mathbf{G}^{(1/2)}\mathbf{G}^{(1/2)}$ ([18], p. 149), [26]. Let

$$\mathbf{R} = \mathbf{G}^{-\frac{1}{2}}\mathbf{A}\mathbf{G}^{-\frac{1}{2}}. \tag{24}$$

Then the matrices $(\sigma^2\mathbf{I}+\mathbf{B})^{-1}\mathbf{A}$ and $\mathbf{R}$ are similar and, hence, their eigenvalues coincide

$$\lambda_j\{(\sigma^2\mathbf{I}+\mathbf{B})^{-1}\mathbf{A}\} = \lambda_j\{\mathbf{R}\} \text{ for } \quad j=1,2,\ldots,m \tag{25}$$

where $\lambda_j\{.\}$ denotes the jth eigenvalue of its matrix argument. Thus, we proceed to examine the joint pdf of the eigenvalues of $\mathbf{R}$. We start by examining the joint pdf of the entries of $\mathbf{R}$.

A. *Distribution of the Elements of* $\mathbf{R}$

The joint pdf of the elements of $\mathbf{R}$ and $\mathbf{G}$ is given by

$$f(\mathbf{R},\mathbf{G}) = J(\mathbf{A},\mathbf{B}\to\mathbf{R},\mathbf{G})f(\mathbf{A},\mathbf{B}) \tag{26}$$

where $J(\mathbf{A},\mathbf{B}\to\mathbf{R},\mathbf{G})$ denotes the Jacobian of the transformation from $\{\mathbf{A},\mathbf{B}\}$ to $\{\mathbf{G},\mathbf{R}\}$. This Jacobian is given by [20]

$$J(\mathbf{A},\mathbf{B}\to\mathbf{R},\mathbf{G}) = \begin{vmatrix} \frac{\partial\mathbf{A}}{\partial\mathbf{G}} & \frac{\partial\mathbf{A}}{\partial\mathbf{R}} \\ \frac{\partial\mathbf{B}}{\partial\mathbf{G}} & \frac{\partial\mathbf{B}}{\partial\mathbf{R}} \end{vmatrix} \tag{27}$$

in terms of the absolute value of the determinant on the right-hand side. In (27), the notation $(\partial\mathbf{A})/(\partial\mathbf{G})$ refers to an $m^2\times m^2$ matrix defined as follows. Introduce the $m^2\times 1$ vectors $\mathbf{a}$ and $\mathbf{g}$

$$\mathbf{a} = \mathsf{vec}(\mathbf{A}) \quad \text{and} \quad \mathbf{g} = \mathsf{vec}(\mathbf{G}) \tag{28}$$

which are obtained by stacking the columns of $\mathbf{A}$ and $\mathbf{G}$. Then the (i,j) element of $(\partial\mathbf{A}/\partial\mathbf{G})$ is given by [23]

$$\left(\frac{\partial\mathbf{A}}{\partial\mathbf{G}}\right)_{i,j} = \frac{\partial a_i}{\partial g_j}, \quad i,j = 1,2,\cdots,m^2 \tag{29}$$

in terms of the derivative of the ith entry of $\mathbf{a}$ with respect to the jth entry of $\mathbf{g}$. Now from $\mathbf{B} = \mathbf{G}-\sigma^2\mathbf{I}$ we get

$$\frac{\partial\mathbf{B}}{\partial\mathbf{G}} = \mathbf{I} \quad \text{and} \quad \frac{\partial\mathbf{B}}{\partial\mathbf{R}} = 0.$$

Substituting these partial derivatives into (27) results in

$$J(\mathbf{A},\mathbf{B}\to\mathbf{R},\mathbf{G}) = \left|\frac{\partial\mathbf{A}}{\partial\mathbf{R}}\right|. \tag{30}$$

Using $\mathbf{A} = \mathbf{G}^{(1/2)}\mathbf{R}\mathbf{G}^{(1/2)}$ we get ([23, p. 183])

$$\left|\frac{\partial\mathbf{A}}{\partial\mathbf{R}}\right| = |\mathbf{G}|^m$$

so that

$$J(\mathbf{A},\mathbf{B}\to\mathbf{R},\mathbf{G}) = |\mathbf{G}|^m \tag{31}$$

Substituting (23) and (31) into (26) gives

$$\begin{aligned} f(\mathbf{R},\mathbf{G}) &= \frac{|\mathbf{G}|^m}{\tilde{\Gamma}_m(s)\tilde{\Gamma}_m(t)} e^{-\mathsf{Tr}(\mathbf{G}^{\frac{1}{2}}\mathbf{R}\mathbf{G}^{\frac{1}{2}}+\mathbf{G}-\sigma^2\mathbf{I})} \\ &\quad \cdot |\mathbf{G}^{\frac{1}{2}}\mathbf{R}\mathbf{G}^{\frac{1}{2}}|^{s-m} \cdot |\mathbf{G}-\sigma^2\mathbf{I}|^{t-m} \\ &= \frac{e^{\mathsf{Tr}\sigma^2\mathbf{I}}}{\tilde{\Gamma}_m(s)\tilde{\Gamma}_m(t)} |\mathbf{R}|^{s-m} \cdot e^{-\mathsf{Tr}\mathbf{G}(\mathbf{R}+\mathbf{I})} \cdot |\mathbf{G}|^s \\ &\quad \cdot |\mathbf{G}-\sigma^2\mathbf{I}|^{t-m} \end{aligned} \tag{32}$$

where we used $\mathsf{Tr}(\mathbf{AB}) = \mathsf{Tr}(\mathbf{BA})$ and $|\mathbf{AB}| = |\mathbf{BA}|$. A more convenient form of the joint pdf can be obtained by using the change of variable $\mathbf{Z} = (1)/(\sigma^2)\mathbf{G}$ (for $\sigma \neq 0$). Then

$$f(\mathbf{R},\mathbf{Z}) = J(\mathbf{G}\to\mathbf{Z})f(\mathbf{R},\mathbf{G}) = \left|\frac{\partial\mathbf{G}}{\partial\mathbf{Z}}\right| f(\mathbf{R},\mathbf{G}) \tag{33}$$

where $|(\partial\mathbf{G})/(\partial\mathbf{Z})| = (\sigma^2)^{2m^2}$ [23], so that (33) becomes

$$f(\mathbf{R},\mathbf{Z}) = (\sigma^2)^{2m^2} f(\mathbf{R},\mathbf{G}). \tag{34}$$

Substituting (32) into (34) results in

$$\begin{aligned} f(\mathbf{R},\mathbf{Z}) &= \frac{(\sigma^2)^{2m^2} e^{\mathsf{Tr}\sigma^2\mathbf{I}}}{\tilde{\Gamma}_m(s)\tilde{\Gamma}_m(t)} |\mathbf{R}|^{s-m} \\ &\quad \cdot e^{-\mathsf{Tr}\sigma^2\mathbf{Z}(\mathbf{R}+\mathbf{I})} \cdot |\sigma^2\mathbf{Z}|^s \cdot |\sigma^2\mathbf{Z}-\sigma^2\mathbf{I}|^{t-m} \\ &= \frac{(\sigma^2)^{s+t-m+2m^2} e^{\mathsf{Tr}\sigma^2\mathbf{I}}}{\tilde{\Gamma}_m(s)\tilde{\Gamma}_m(t)} |\mathbf{R}|^{s-m} \\ &\quad \cdot e^{-\mathsf{Tr}\mathbf{Z}[\sigma^2(\mathbf{R}+\mathbf{I})]} \cdot |\mathbf{Z}|^s \cdot |\mathbf{Z}-\mathbf{I}|^{t-m} \\ &= \frac{c}{\tilde{\Gamma}_m(s)\tilde{\Gamma}_m(t)} |\mathbf{R}|^{s-m} \\ &\quad \cdot e^{-\mathsf{Tr}\mathbf{Z}[\sigma^2(\mathbf{R}+\mathbf{I})]} \cdot |\mathbf{Z}|^s \cdot |\mathbf{Z}-\mathbf{I}|^{t-m} \end{aligned} \tag{35}$$

where c is a constant that depends on σ^2. We can now obtain $f(\mathbf{R})$ from $f(\mathbf{R},\mathbf{Z})$ by integrating with respect to $\mathbf{Z}$

$$f(\mathbf{R}) = \int_{\mathbf{Z}} f(\mathbf{R},\mathbf{Z})d\mathbf{Z}$$

Note that $\mathbf{Z} > \mathbf{I}$, so that $\mathbf{Z}-\mathbf{I}$ is a positive definite matrix. It follows that

$$\begin{aligned} f(\mathbf{R}) &= \int_{\mathbf{Z}>\mathbf{I}} f(\mathbf{R},\mathbf{Z})d\mathbf{Z} \\ &= \int_{\mathbf{Z}>\mathbf{I}} \frac{c}{\tilde{\Gamma}_m(s)\tilde{\Gamma}_m(t)}|\mathbf{R}|^{s-m} \\ &\quad \cdot e^{-\mathrm{Tr}\mathbf{Z}[\sigma^2(\mathbf{R}+\mathbf{I})]}\cdot|\mathbf{Z}|^s\cdot|\mathbf{Z}-\mathbf{I}|^{t-m}d\mathbf{Z} \\ &= \frac{c}{\tilde{\Gamma}_m(s)\tilde{\Gamma}_m(t)}|\mathbf{R}|^{s-m} \\ &\quad \cdot\int_{\mathbf{Z}>\mathbf{I}} e^{-\mathrm{Tr}\mathbf{Z}[\sigma^2(\mathbf{R}+\mathbf{I})]}\cdot|\mathbf{Z}|^s\cdot|\mathbf{Z}-\mathbf{I}|^{t-m}d\mathbf{Z} \\ &= \frac{c}{\tilde{\Gamma}_m(s)\tilde{\Gamma}_m(t)}|\mathbf{R}|^{s-m} \\ &\quad \cdot\int_{\mathbf{Z}>\mathbf{I}} e^{-\mathrm{Tr}(\mathbf{Z}\mathbf{\Theta})}\cdot|\mathbf{Z}|^s\cdot|\mathbf{Z}-\mathbf{I}|^{t-m}d\mathbf{Z} \end{aligned} \tag{36}$$

where $\mathbf{\Theta} = \sigma^2(\mathbf{R}+\mathbf{I})$. In order to evaluate the integration in (36), we resort to the definition of the Whittaker function of a complex matrix argument, $W_{\alpha,\beta}(\mathbf{\Theta})$, introduced in [23]. For an $m\times m$ complex matrix $\mathbf{Z}$, the Whittaker function is defined via[1]

$$\begin{aligned} W_{\alpha,\beta}(\mathbf{\Theta}) &= \frac{|\mathbf{\Theta}|^{\beta+\frac{m}{2}}\cdot e^{-\frac{1}{2}\mathrm{Tr}\mathbf{\Theta}}}{\tilde{\Gamma}_m(\beta-\alpha+m/2)} \\ &\quad \cdot\int_{\mathbf{T}>\mathbf{0}} e^{-\mathrm{Tr}(\mathbf{T}\mathbf{\Theta})}\cdot|\mathbf{T}|^{\beta-\alpha-\frac{m}{2}}\cdot|\mathbf{T}+\mathbf{I}|^{\beta+\alpha-\frac{m}{2}}d\mathbf{T} \end{aligned} \tag{37}$$

where α and β are generally complex parameters. In order to reduce (37) to a form similar to (36), we let $\mathbf{T}=\mathbf{Z}-\mathbf{I}$ so that

$$J(\mathbf{Z}\to\mathbf{T}) = \mathbf{I}. \tag{38}$$

Substituting into (37) we get

$$\begin{aligned} W_{\alpha,\beta}(\mathbf{\Theta}) &= \frac{|\mathbf{\Theta}|^{\beta+\frac{m}{2}}\cdot e^{-\frac{1}{2}\mathrm{Tr}\mathbf{\Theta}}}{\tilde{\Gamma}_m(\beta-\alpha+m/2)} \\ &\quad \cdot\int_{\mathbf{Z}>\mathbf{I}} e^{-\mathrm{Tr}(\mathbf{Z}-\mathbf{I})\mathbf{\Theta}}\cdot|\mathbf{Z}-\mathbf{I}|^{\beta-\alpha-\frac{m}{2}}\cdot|\mathbf{Z}|^{\beta+\alpha-\frac{m}{2}}d\mathbf{Z} \end{aligned}$$

i.e.,

$$\begin{aligned} W_{\alpha,\beta}(\mathbf{\Theta}) &= \frac{|\mathbf{\Theta}|^{\beta+\frac{m}{2}}\cdot e^{\frac{1}{2}\mathrm{Tr}\mathbf{\Theta}}}{\tilde{\Gamma}_m(\beta-\alpha+m/2)} \\ &\quad \cdot\int_{\mathbf{Z}>\mathbf{I}} e^{-\mathrm{Tr}(\mathbf{Z}\mathbf{\Theta})}\cdot|\mathbf{Z}-\mathbf{I}|^{\beta-\alpha-\frac{m}{2}}\cdot|\mathbf{Z}|^{\beta+\alpha-\frac{m}{2}}d\mathbf{Z}. \end{aligned} \tag{39}$$

Comparing with the expression for $f(\mathbf{R})$ in (36), we see that if we select

$$\alpha = \frac{1}{2}(s-t+m) \quad \text{and} \quad \beta = \frac{1}{2}(s+t) \tag{40}$$

then we can relate $f(\mathbf{R})$ and $W_{\alpha,\beta}(\mathbf{\Theta})$ as follows:

$$\begin{aligned} f(\mathbf{R}) &= \frac{c}{\tilde{\Gamma}_m(s)}\cdot\frac{|\mathbf{R}|^{s-m}}{|\sigma^2(\mathbf{R}+\mathbf{I})|^{\frac{1}{2}(t+s-m)}} \\ &\quad \cdot e^{-\frac{1}{2}\mathrm{Tr}\sigma^2(\mathbf{R}+\mathbf{I})}\cdot W_{\alpha,\beta}(\sigma^2(\mathbf{R}+\mathbf{I})). \end{aligned} \tag{41}$$

[1]See [27], [28] for the definition of the Whittaker function for scalar arguments and for real matrix arguments.

We have therefore derived an expression for the joint pdf of the elements of the matrix $\mathbf{R}$ of (24) in terms of the Whittaker function of the argument $\sigma^2(\mathbf{R}+\mathbf{I})$. We now proceed to examine the distribution of the eigenvalues of $\mathbf{R}$.

B. Distribution of the Eigenvalues of $\mathbf{R}$

Introduce eigenvalue decomposition of the matrix $\mathbf{R}$, say

$$\mathbf{R} = \mathbf{U}\mathbf{\Lambda}\mathbf{U}^* \tag{42}$$

where $\Lambda = \mathrm{diag}\{\lambda_1,\lambda_2,\ldots,\lambda_m\}$ and $\mathbf{U}$ is unitary. Then,

$$\begin{aligned} |\mathbf{R}| &= \prod_{j=1}^{m}|\lambda_j|, \quad |\sigma^2(\mathbf{R}+\mathbf{I})| = \prod_{j=1}^{m}|\sigma^2(\lambda_j+1)| \\ \mathrm{Tr}\mathbf{R} &= \sum_{j=1}^{m}\lambda_j, \quad \mathrm{Tr}\sigma^2(\mathbf{R}+\mathbf{I}) = \sum_{j=1}^{m}\sigma^2(\lambda_j+1). \end{aligned} \tag{43}$$

Also, consider the eigen-decomposition of the matrix $\mathbf{\Theta} = \sigma^2(\mathbf{R}+\mathbf{I})$, say

$$\mathbf{\Theta} = \tilde{\mathbf{U}}\tilde{\mathbf{\Lambda}}\tilde{\mathbf{U}}^*. \tag{44}$$

Actually, $\tilde{\mathbf{U}} = \mathbf{U}$ and $\tilde{\mathbf{\Lambda}} = \sigma^2(\mathbf{\Lambda}+\mathbf{I})$. Then, from (37) and after some simplifications,

$$\begin{aligned} W_{\alpha,\beta}(\mathbf{\Theta}) &= \frac{|\tilde{\mathbf{\Lambda}}|^{\beta+\frac{m}{2}}\cdot e^{-\frac{1}{2}\mathrm{Tr}\tilde{\mathbf{\Lambda}}}}{\tilde{\Gamma}_m(\beta-\alpha+m/2)} \\ &\times\int_{\mathbf{T}>\mathbf{0}} e^{-\mathrm{Tr}(\mathbf{T}\tilde{\mathbf{U}}\tilde{\mathbf{\Lambda}}\tilde{\mathbf{U}}^*)}\cdot|\mathbf{T}|^{\beta-\alpha-\frac{m}{2}}\cdot|\mathbf{T}+\mathbf{I}|^{\beta+\alpha-\frac{m}{2}}d\mathbf{T}. \end{aligned} \tag{45}$$

Introduce the change of variable $\mathbf{F} = \tilde{\mathbf{U}}^*\mathbf{T}\tilde{\mathbf{U}}$. It follows that the Jacobian of this transformation is given by

$$J(\mathbf{T}\to\mathbf{F}) = |\tilde{\mathbf{U}}|^{2m} = 1^{2m} = 1. \tag{46}$$

Since $\mathbf{T}$ is positive definite, it also follows that $\mathbf{F}$ is positive definite. Then (45) becomes

$$\begin{aligned} W_{\alpha,\beta}(\mathbf{\Theta}) &= \frac{|\tilde{\mathbf{\Lambda}}|^{\beta+\frac{m}{2}}e^{-\frac{1}{2}\mathrm{Tr}\tilde{\mathbf{\Lambda}}}}{\tilde{\Gamma}_m(\beta-\alpha+m/2)}\int_{\mathbf{F}>0} e^{-\mathrm{Tr}(\mathbf{F}\tilde{\mathbf{\Lambda}})} \\ &\quad \cdot|\mathbf{F}|^{\beta-\alpha-\frac{m}{2}}\cdot|\mathbf{F}+\mathbf{I}|^{\beta+\alpha-\frac{m}{2}}d\mathbf{F} = W_{\alpha,\beta}(\tilde{\mathbf{\Lambda}}). \end{aligned} \tag{47}$$

In other words

$$\begin{aligned} W_{\alpha,\beta}\left(\sigma^2(\mathbf{R}+\mathbf{I})\right) &= W_{\alpha,\beta}(\mathbf{\Theta}) = W_{\alpha,\beta}(\tilde{\mathbf{\Lambda}}) \\ &= W_{\alpha,\beta}[\sigma^2(\mathbf{\Lambda}+\mathbf{I})] \end{aligned} \tag{48}$$

so that we may replace $\mathbf{R}$ by $\mathbf{\Lambda}$ as an argument for $W_{\alpha,\beta}(.)$. Now to obtain the joint pdf of $\{\lambda_1,\lambda_2,\ldots,\lambda_m\}$ from $f(\mathbf{R})$, the Jacobian of the transformation from $\mathbf{R}$ to the $\{\lambda_i\}$ is given by [23]

$$\begin{aligned} &J(\mathbf{R}\to\{\lambda_1,\lambda_2,\ldots,\lambda_m\},\mathbf{U}) \\ &\qquad = \frac{\pi^{m(m-1)}}{\tilde{\Gamma}_m(m)}\prod_{\substack{l,j=1\\ l<j}}^{l,j=m}|\lambda_l-\lambda_j|^2. \end{aligned} \tag{49}$$

Using (43) and (49) in (41) results in the desired expression

$$f(\{\lambda_1,\lambda_2,\ldots,\lambda_m\},\mathbf{U}) = \frac{c\pi^{m(m-1)}}{\tilde{\Gamma}_m(s)\tilde{\Gamma}_m(t)\tilde{\Gamma}_m(m)}\left(\prod_{\substack{l,j=1\\ l<j}}^{l,j=m}|\lambda_l-\lambda_j|^2\right) \cdot\left(\prod_{j=1}^{m}\frac{|\lambda_j|^{s-m}e^{-\frac{1}{2}\sigma^2(\lambda_j+1)}}{|\sigma^2(\lambda_j+1)|^{\frac{1}{2}(t+s-m)}}W_{\alpha,\beta}[\sigma^2(\mathbf{\Lambda}+\mathbf{I})]\right). \tag{50}$$

In order to obtain an expression for $f(\mathbf{\Lambda})$, the pdf in (51), shown at the bottom of the page, is integrated over $\mathbf{U}$. It can be shown that $\int_{\mathbf{U}} d\mathbf{U}=\alpha$ where α is a constant ([29, p. 33], [30, p. 361]). Finally, the joint pdf of the eigenvalues is given by

$$f(\lambda_1,\lambda_2,\ldots,\lambda_m) = C\left(\prod_{\substack{l,j=1\\ l<j}}^{l,j=m}|\lambda_l-\lambda_j|^2\right) \cdot\left(\prod_{j=1}^{m}\frac{|\lambda_j|^{s-m}e^{-\frac{1}{2}\sigma^2(\lambda_j+1)}}{|\sigma^2(\lambda_j+1)|^{\frac{1}{2}(t+s-m)}}W_{\alpha,\beta}[\sigma^2(\mathbf{\Lambda}+\mathbf{I})]\right) \tag{52}$$

where

$$C=\frac{\alpha\cdot c\cdot\pi^{m(m-1)}}{\tilde{\Gamma}_m(s)\tilde{\Gamma}_m(t)\tilde{\Gamma}_m(m)}.$$

We have therefore arrived at an expression for the joint pdf of the eigenvalues of the matrix combination $(\sigma^2\mathbf{I}+\tilde{\mathbf{\Phi}}^*\tilde{\mathbf{\Phi}})^{-1}\mathbf{\Phi}^*\mathbf{\Phi}$. The result is in terms of a Whittaker function, which is defined by means of the integral (47).

In the case of a scalar argument, the Whittaker function can be expressed in terms of confluent hypergeometric functions [23], which can be numerically approximated as in [31]. We now explain how an approximation for $W_{\alpha,\beta}[\sigma^2(\mathbf{\Lambda}+\mathbf{I})]$ can be used to get some insight into the behavior of the pdf expression (53). In Appendix A we argue that for small values of σ^2, the Whittaker matrix function can be approximated by

$$W_{\alpha,\beta}(\mathbf{X})\approx \mathbf{k}\mathbf{e}^{-\frac{1}{2}\mathsf{Tr}\mathbf{x}}|\mathbf{X}|^{\left(\frac{\mathbf{m}}{2}-\beta\right)}$$

for some constant k. In this case, the joint pdf of the eigenvalues in (52) becomes

$$f(\lambda_1,\lambda_2,\ldots,\lambda_m)\approx c\left(\prod_{\substack{l,j=1\\ l<j}}^{l,j=m}|\lambda_l-\lambda_j|^2\right) \cdot\left(\prod_{j=1}^{m}\frac{|\lambda_j|^{s-m}e^{-\sigma^2(\lambda_j+1)}}{|\sigma^2(\lambda_j+1)|^{(s+t)}}\right) \tag{53}$$

for some constant c.

The joint pdf of the eigenvalues of $(\tilde{\mathbf{\Phi}}^*\tilde{\mathbf{\Phi}})^{-1}\mathbf{\Phi}^*\mathbf{\Phi}$, which corresponds to the special case $\sigma^2=0$, and also requires $\tilde{\mathbf{\Phi}}$ to be full rank, was studied in [24], [32]. Referred to as β-Jacobi ensemble, the joint pdf of the eigenvalues was given in [32] as

$$f(\lambda_1,\lambda_2,\ldots,\lambda_m)\propto\left(\prod_{\substack{l,j=1\\ l<j}}^{l,j=m}|\lambda_l-\lambda_j|^2\right) \cdot\left(\prod_{j=1}^{m}\frac{|\lambda_j|^{s-m}}{|(\lambda_j+1)|^{(s+t)}}\right). \tag{54}$$

Note that the expression in (53) covers (54) as a special case for $\sigma^2=0$.

Finally, the pdf of the maximum eigenvalue, $\lambda_{\max}$, can be obtained by integrating the joint pdf in (53) over the other eigenvalues (see (55), shown at the bottom of the page). In order to plot $f(\lambda_{\max};s,t,m)$, the integration in (55) is performed numerically. Fig. 4(a) and (b) shows the histograms of $\lambda_{\max}$ that are obtained by simulation and by using the pdf expression given

$$\begin{aligned} f(\{\lambda_1,\lambda_2,\ldots,\lambda_m\}) &= \int_{\mathbf{U}} f(\{\lambda_1,\lambda_2,\ldots,\lambda_m\},\mathbf{U})d\mathbf{U}\\ &= \frac{c\pi^{m(m-1)}}{\tilde{\Gamma}_m(s)\tilde{\Gamma}_m(t)\tilde{\Gamma}_m(m)}\left(\prod_{\substack{l,j=1\\ l<j}}^{l,j=m}|\lambda_l-\lambda_j|^2\right)\cdot\left(\prod_{j=1}^{m}\frac{|\lambda_j|^{s-m}e^{-\frac{1}{2}\sigma^2(\lambda_j+1)}}{|\sigma^2(\lambda_j+1)|^{\frac{1}{2}(t+s-m)}}W_{\alpha,\beta}[\sigma^2(\mathbf{\Lambda}+\mathbf{I})]\right)\int_{\mathbf{U}} d\mathbf{U}. \end{aligned} \tag{51}$$

$$f(\lambda_{\max};s,t,m)\propto\int_{\lambda_2=0}^{\lambda_{\max}}\int_{\lambda_3=0}^{\lambda_2}\cdots\int_{\lambda_{m-1}=0}^{\lambda_N}f(\lambda_1,\ldots,\lambda_m;s,t,m)d\lambda_2 d\lambda_3\ldots d\lambda_m. \tag{55}$$

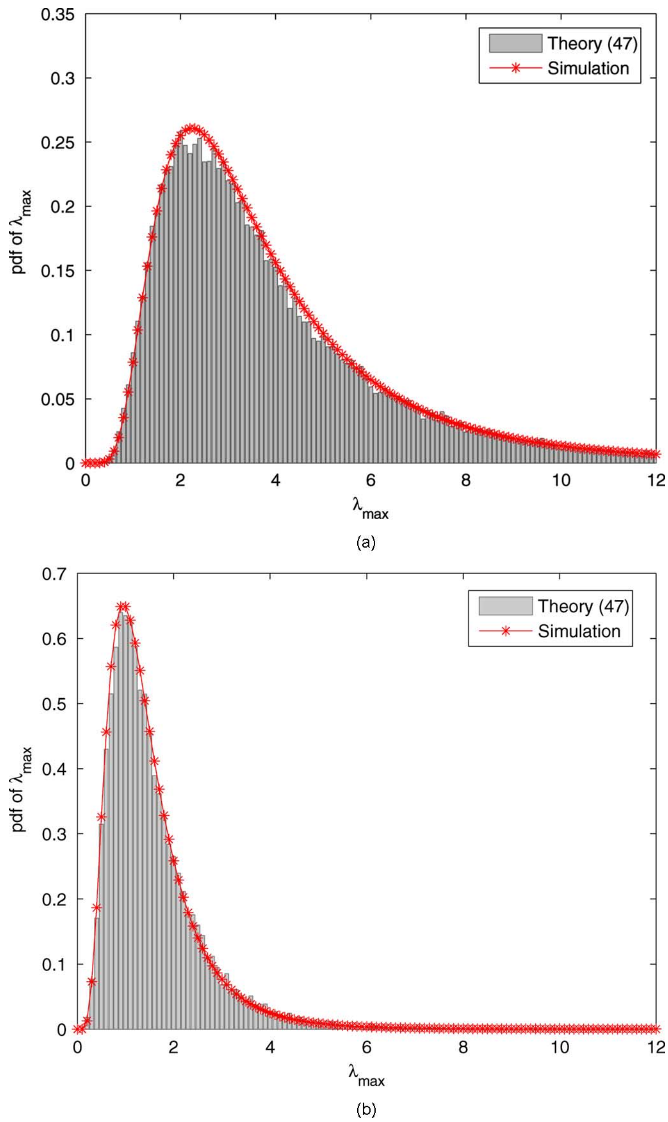

Fig. 4. Probability density function of $\lambda_{\max}$ obtained by simulation and by using (53) for (a) $m = 3$, $s = 4$, $t = 5$ and $\sigma^2 = 0.3$. (b) $m = 2$, $s = 4$, $t = 6$ and $\sigma_i^2 = 0.2$.

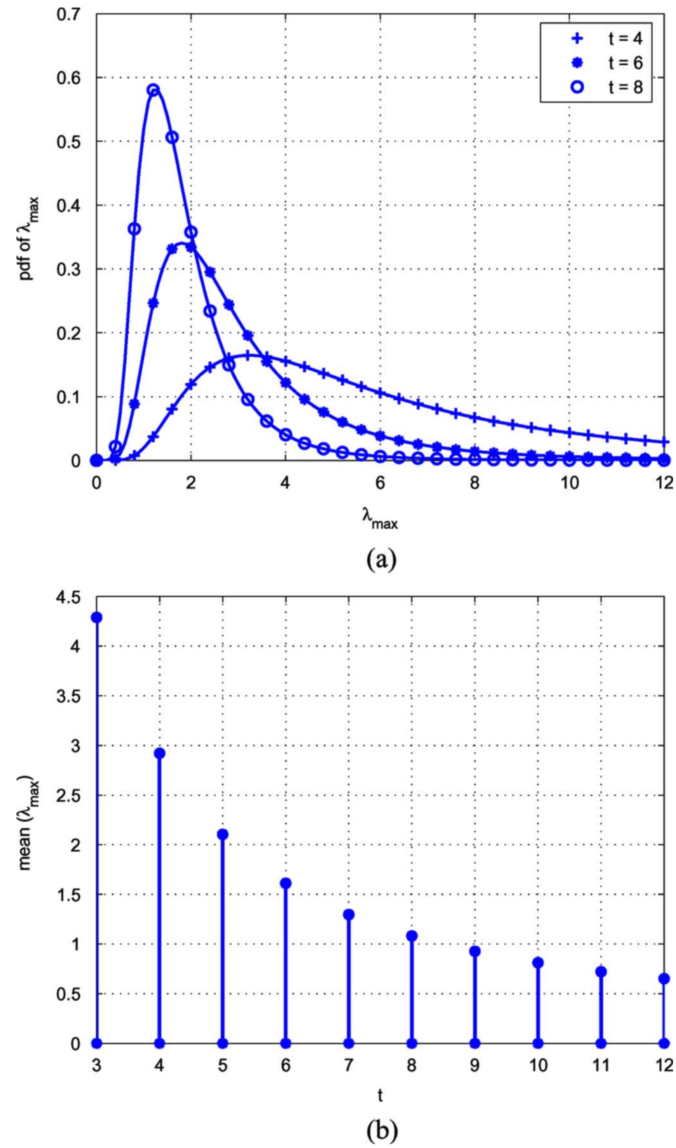

Fig. 5. Probability density function of $\lambda_{\max}$ obtained by simulation and by using (53) for (a) the derived pdf of $\lambda_{\max}$ for $m = 2$, $s = 4$, $\sigma^2 = 0.2$, and three values of $t = \{4, 6, 8\}$. (b) Mean value of $\lambda_{\max}$ versus t for fixed values of m, s, and $\sigma^2 = 0.2$.

by (53). It is clear that the theoretical distribution matches well with the simulated histogram.

IV. Antenna Selection Procedure

We now show how the results of the previous section can be used to decide on antenna selection in a downlink multiuser MIMO environment. Thus, recall that $s = M_i, m = N$, and $t = \sum_{\substack{j=1 \\ j\neq i}}^{K} M_j$, so that the joint pdf of the eigenvalues of $(M_i\sigma_i^2\mathbf{I} + \tilde{\mathbf{H}}_i^*\tilde{\mathbf{H}}_i)^{-1}\mathbf{H}_i^*\mathbf{H}_i$ is given by [cf. (53)]

$$f(\lambda_1, \ldots, \lambda_N; N, \{M_i\}) \propto \left(\prod_{\substack{l<j \\ l,j=1}}^{l,j=m} |\lambda_l - \lambda_j|^2 \right) \cdot \left(\prod_{j=1}^{N} \frac{|\lambda_j|^{M_i - N} e^{-M_i\sigma_i^2(\lambda_j+1)}}{|M_i\sigma^2(\lambda_j+1)|^{(\sum_{j=1}^{K} M_j)}} \right). \quad (56)$$

Recall from (14) that optimal SLNR $= \lambda_{\max}$. Thus, a higher $\lambda_{\max}$ or SLNR translates into less CCI and better system performance.

In Fig. 5(a), the pdf of $\lambda_{\max}$ for different values of t (or $\sum_{\substack{j=1 \\ j\neq i}}^{K} M_j$) is shown. As t increases (i.e., as the total number of antennas by all other users increases), the pdf curve shifts to the left indicating a decrease in the average value of $\lambda_{\max}$. The figure also shows that the variance (which measures the spread around the mean) of $\lambda_{\max}$ increases as t decreases. Fig. 5(b) shows the mean value of $\lambda_{\max}$ for different values of t. These results suggest the interesting conclusion that the CCI is enhanced as the total number of active antennas at all other users increases. In other words, for a fixed M_i, increasing $\sum_{\substack{j=1 \\ j\neq i}}^{K} M_j$ would increase the CCI and hence degrade the overall system performance. In the same token, reducing the number of active antennas at one user helps the other users in the system. Note that this result is specific to the SLNR criterion. This is due to the suboptimality of the solution with respect to the SINR criterion. This conclusion suggests a dynamic method for antenna selection that would improve system performance. According to the proposed scheme, we reduce the number of active antennas for users not meeting an SINR threshold. The threshold value applies to the SINR at the output of the receiver. By lowering the number of antennas for these users, the other users in the network will have a higher probability to meet their SINR threshold. This procedure does not yield any degradation in the system performance in terms of outage values since those users not meeting the SINR threshold cannot establish a connection anyway. Thus, for each channel realization, we perform a search over all possible receive antenna combinations $(2^{\sum_i M_i} - 1)$ and choose the combination that results in a maximum number of users meeting an SINR threshold. In general, there may be more than one combination of receive antennas that fulfill this condition. Thus, among all combinations, we choose the one that maximizes the SINR of the worst above-the-threshold user. This scheme does not require any change in the receivers; it simply implies that the receiver should only consider the signals received at the active antennas when estimating the received signal. In the cases that some users are meeting their SINR threshold by a large margin, their number of active antennas can be reduced in favor of other users in the system. As long as such users still meet their threshold, the reduction in their active antennas will help the other users in the system. Overall, this mechanism can statistically improve the outage results for all users in the network.

Although exhaustive search is not efficient from the complexity point of view, the purpose of this paper is to show that, in principle and in theory, the proposed selection scheme makes a significant difference. Other suboptimal schemes can be considered where an antenna elimination algorithm is developed to gradually eliminate receive antennas from the users with the best SINR until the maximum number possible of users are above their SINR thresholds.

V. Simulations

In the simulation environment, we assume the ith user estimates s_i from $\mathbf{y}_i$ in (4) according to a classical single-user maximum-likelihood detection scheme (without relying on knowledge of the other channels), i.e.,

$$\hat{s}_i \triangleq \frac{\mathbf{w}_i^* \mathbf{H}_i^* \mathbf{y}_i}{\|\mathbf{H}_i \mathbf{w}_i\|^2}.$$

The simulation results are shown in Figs. 6 and 7. These figures compare the final SINR outage curves for the following two scenarios: 1) all the available number of antennas for all users are used; 2) the configuration suggested by the search scheme of Section IV is used. For further insight, the distribution of the number of active antennas for each user as well as the total active receive antennas are plotted. The channel model described in Section II is used in all simulations, where every channel path has a complex Gaussian distribution independent of the other paths. Two different configurations are simulated.

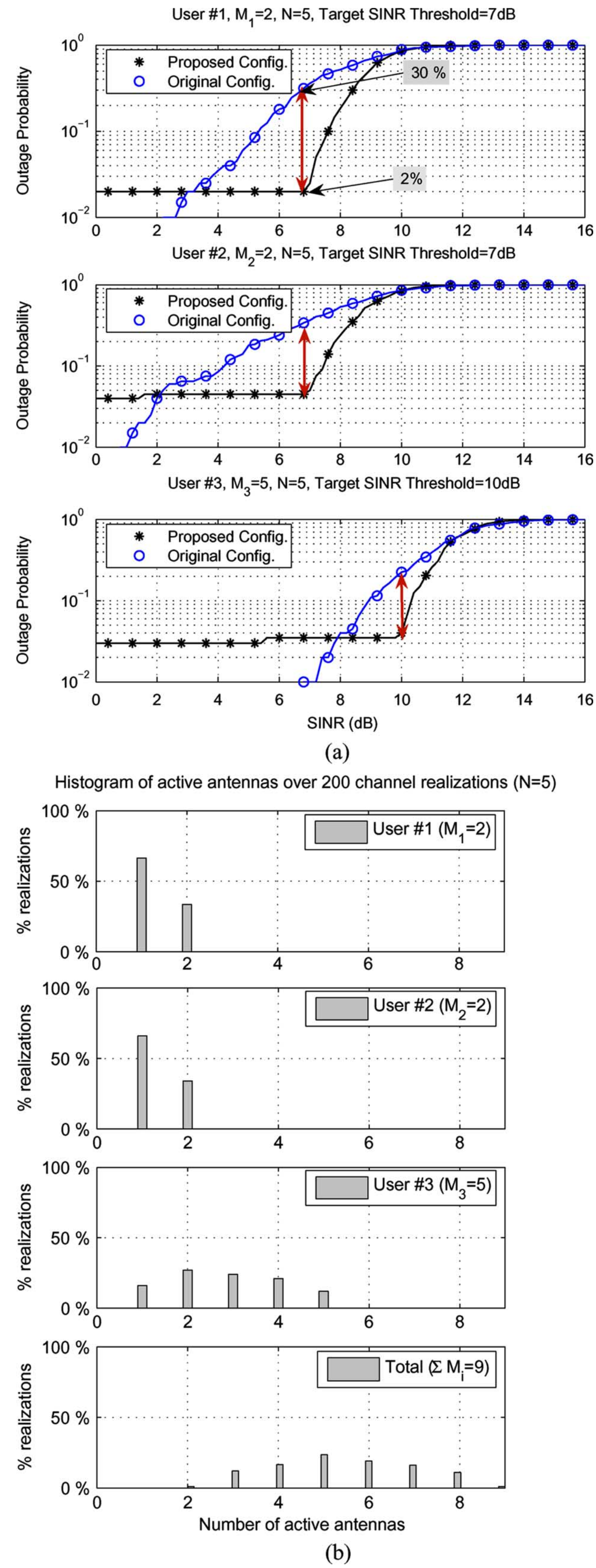

Fig. 6. (a) SINR outage probability for all the users. (b) Distribution of the number active receive antennas for each user after applying the proposed scheme. $10\log_{10} 1/\sigma^2 = 0$ for all users.

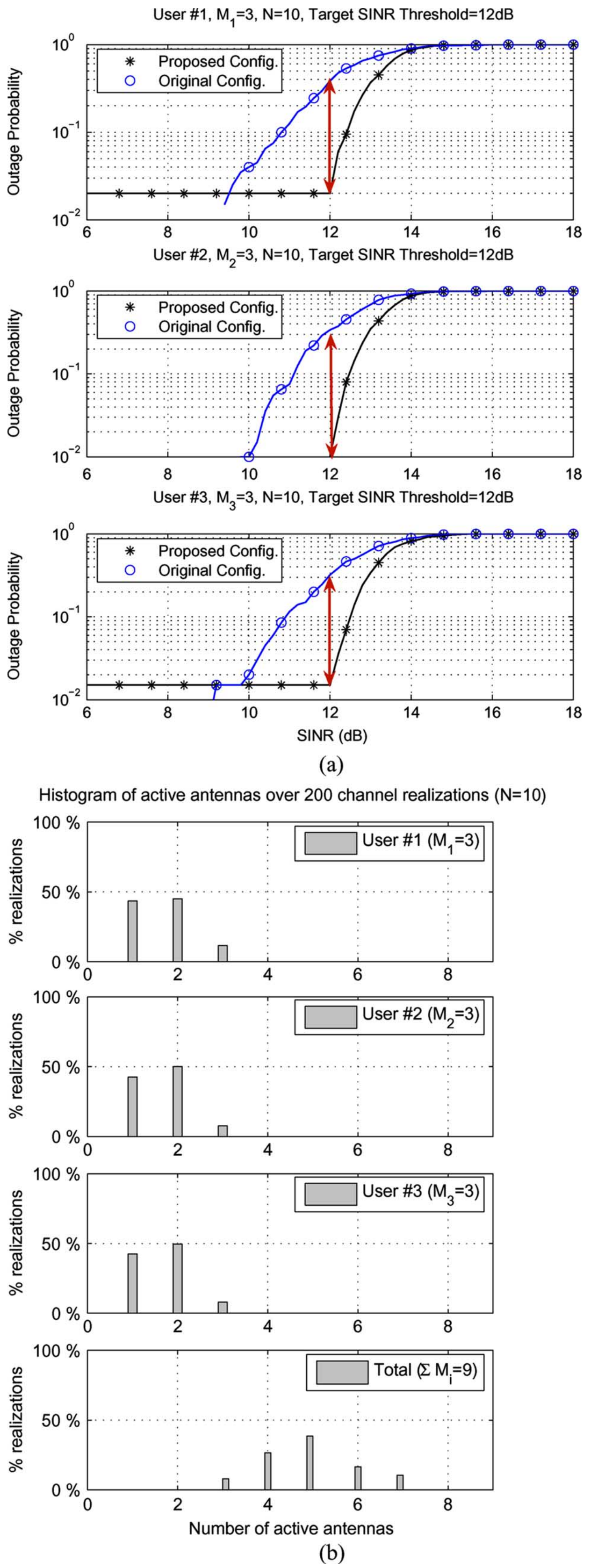

Fig. 7. (a) SINR outage probability for all the users. (b) Distribution of the number active receive antennas for each user after applying the proposed scheme. $10\log_{10} 1/\sigma^2 = 0$ for all users.

A. $\mathbf{H}_i$ and $\tilde{\mathbf{H}}_i$ are Tall Matrices

$\sum_{j\neq i} M_j > N$

- number of transmit antennas $N = 5$
- number of users $K = 3$
- number of available receive antennas $\{M_1, M_2, M_3\} = \{2, 2, 5\}$
- target SINR thresholds $\{T_1, T_2, T_3\} = \{7, 7, 10\}$dB.

The SINR per received antenna is defined as $1/\sigma_i^2$ and is assumed to be 0 dB. The simulation is conducted over 200 channel realizations.

Fig. 6(a) shows the resulting outage curves for each of the 3 users in the system for the following 2 cases:

- using all available antennas;
- using the proposed antenna configuration.

The curves in Fig. 6(a) are SINR outage curves. That is, each curve is the cumulative density function (cdf) of the SINR at the output of the receiver for the corresponding user. The outage curve represents $P(\mathsf{SINR} \leq \mu)$ on the vertical axis for different values of μ on the horizontal axis. Consider the results for user 1 in the top plot of Fig. 6(a). The SINR threshold for this user is 7 dB meaning that if the SINR value for this user falls below 7 dB, the package is dropped and it has to be re-transmitted. Thus, the probability $P(\mathsf{SINR} \leq 7\text{ dB})$ measures the likelihood that this user will not establish communication with the transmitter. The figure shows that by using the original antenna configuration, user 1 achieves an outage of 30% while using the proposed scheme the outage reduces to 2%. Note that the curve for the proposed scheme is flat for SINR values up to the threshold (7 dB) and then it increases. This is because in our proposed scheme, the signal is transmitted to the user only if there is a reliable channel (i.e., if the SINR is above the threshold). This hard decision at the transmitter translates into the breakpoint in the curve. Thus the flat part of the curve corresponds to the case of no transmission and its value is the outage percentage for all the values of SINR below the threshold.

According to the results shown in Fig. 6(a), the following outage improvements are achieved:

- user 1 (7 dB outage): from 30% to 2%
- user 2 (7 dB outage): from 40% to 5%
- user 3 (10 dB outage): from 20% to 3%.

Thus all three users experience a significant improvement in outage probability at their target SINR.

For this antenna configuration, it can be seen from Fig. 6(a) that the SINR of the users are sacrificed in the region where SINR is below the target threshold. This yields no degradation in the target SINR outage since no reliable communication is desired below this threshold anyways. However, by sacrificing the SINR of one users, the other users meet their thresholds with a greater probability, as was argued in Section IV. It can also be seen from Fig. 6(b) that the optimum choice for number of active users can be different from the original available number of receive antennas.

Fig. 6(b) shows the histogram of the number of selected active antennas for each user over 200 channel realizations. Consider user 1 for example; this user has 2 receive antennas. The figure shows that out of the 2 antennas, only 1 is active 65% of the time while both antennas are active only 35% of the time as compared

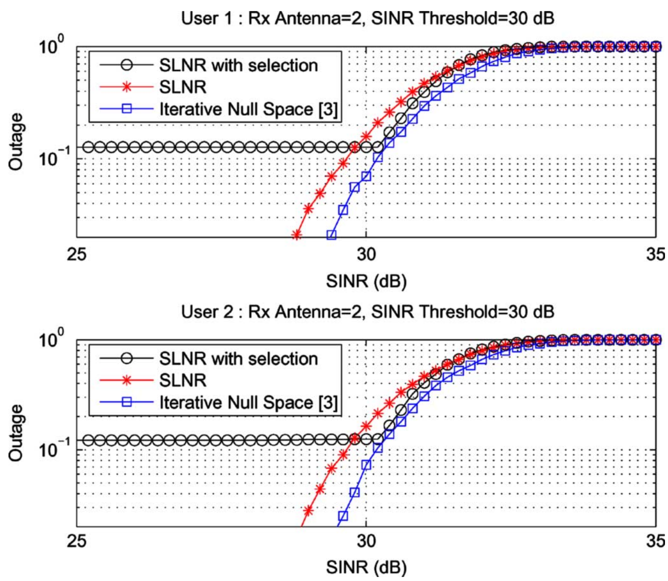

Fig. 8. Outage versus SINR for 2 users each having 2 receive antennas for a system with 12 transmit antennas. The SINR thresholds are $\{30, 30\}$ dB.

to the original configuration where the 2 receive antennas are active 100% of the time.

B. $\mathbf{H}_i$ and $\tilde{\mathbf{H}}_i$ are Fat Matrices

$\sum_{j\neq i} M_j < N$

- number of transmit antennas $N = 10$
- number of users $K = 3$
- number of available receive antennas $\{M_1, M_2, M_3\} = \{3, 3, 3\}$
- target SINR thresholds $\{T_1, T_2, T_3\} = \{12, 12, 12\}$ dB.

According to the results shown in Fig. 7(a), the following outage improvements are achieved:

- user 1 (12 dB outage): from 40% to 2%
- user 2 (12 dB outage): from 30% to 1%
- user 3 (12 dB outage): from 30% to 1.6%.

Fig. 7(b) shows the histogram of the selected active antennas for each user for this configuration.

C. SLNR-Based Antenna Selection Versus Iterative SINR Solution

Fig. 8 shows the SINR outage curves for the following antenna configuration: $N = 12$, $M_i = 2$, SINR threshold $=$ 30 dB and $1/\sigma_i^2 = 20$ dB. The figure compares three schemes:

1) the SLNR-based scheme without antenna selection;
2) the SLNR-based scheme combined with antenna selection; this is the scheme we propose in this paper;
3) the iterative scheme proposed in [3].

The figure shows that the SLNR-based scheme performs within less than 1 dB of the iterative scheme. The proposed antenna selection further improves the SLNR-based scheme to achieve a performance that approaches that of the iterative solution in [3]. Fig. 8 further ahead.

VI. Conclusion

We have proposed a dynamic antenna scheduling strategy for downlink MIMO communications that is based on characterizing and exploiting the dependence of the signal-to-leakage-plus-noise (SLNR) ratio on the system parameters. The SLNR strategy is found to relax the condition on the number of transmit-receive antennas in comparison to traditional zero-forcing and time-scheduling strategies. It was shown that the largest value that the SLNR can achieve is equal to the maximum eigenvalue of a certain channel-dependent random matrix combination. The pdf of the maximum eigenvalue was further characterized in terms of a Whittaker function and the result was used to show that increasing the number of antennas at some users can degrade the SLNR performance at other users. This fact was exploited to propose an antenna scheduling scheme that leads to significant improvement in terms of SINR outage probabilities. Simulation results illustrate the resulting system performance.

Appendix A
Whittaker Matrix Function Approximation

In this section, we derive an approximation for the Whittaker matrix function for a small complex matrix argument. To begin with, we note that for any Hermitian matrix $\mathbf{X}$

$$e^{-\mathsf{Tr}\mathbf{x}} = \mathsf{det}(e^{-\mathbf{X}}) = |e^{-\mathbf{X}}| \tag{57}$$

where for the second equality we recall our convention that the notation $|\cdot|$ denotes the absolute value of the determinant of its argument (and $\mathsf{det}(e^{-\mathbf{X}}) > 0$ for any $\mathbf{X}$). When $\|\mathbf{X}\| < 1$, we may write the power series expansion

$$e^{\mathbf{X}} = \sum_{n=0}^{\infty} \frac{\mathbf{X}^n}{n!} \approx \mathbf{I} + \mathbf{X} \quad \text{for } \|\mathbf{X}\| \to 0. \tag{58}$$

Thus, for small enough $\mathbf{X}$, we have

$$e^{-\mathsf{Tr}\mathbf{x}} \approx |\mathbf{I} - \mathbf{X}|. \tag{59}$$

Now consider the Whittaker function from (37):

$$W_{\alpha,\beta}(\mathbf{\Theta}) = \frac{|\mathbf{\Theta}|^{\beta+\frac{m}{2}} \cdot e^{-\frac{1}{2}\mathsf{Tr}\mathbf{\Theta}}}{\tilde{\Gamma}_m(\beta - \alpha + m/2)} \cdot \int_{\mathbf{T}>0} e^{-\mathsf{Tr}(\mathbf{T}\mathbf{\Theta})} \cdot |\mathbf{T}|^{\beta-\alpha-\frac{m}{2}} \cdot |\mathbf{T}+\mathbf{I}|^{\beta+\alpha-\frac{m}{2}} d\mathbf{T}. \tag{60}$$

For $\|\mathbf{\Theta}\| \to 0$, we have

$$\begin{aligned}\int_{\mathbf{T}>0} & e^{-\mathsf{Tr}(\mathbf{T}\mathbf{\Theta})} \cdot |\mathbf{T}|^{\beta-\alpha-\frac{m}{2}} \cdot |\mathbf{T}+\mathbf{I}|^{\beta+\alpha-\frac{m}{2}} d\mathbf{T} \\ &\approx \int_{\mathbf{T}>0} |\mathbf{I} - \mathbf{T}\mathbf{\Theta}| \cdot |\mathbf{T}|^{\beta-\alpha-\frac{m}{2}} \cdot |\mathbf{T}+\mathbf{I}|^{\beta+\alpha-\frac{m}{2}} d\mathbf{T} \\ &= \int_{\mathbf{T}>0} |\mathbf{I} - \mathbf{\Theta}^{\frac{*}{2}}\mathbf{T}\mathbf{\Theta}^{\frac{1}{2}}| \cdot |\mathbf{T}|^{\beta-\alpha-\frac{m}{2}} \cdot |\mathbf{T}+\mathbf{I}|^{\beta+\alpha-\frac{m}{2}} d\mathbf{T}\end{aligned} \tag{61}$$

where in (61), we introduced the square root decomposition of $\mathbf{\Theta}$, i.e., $\mathbf{\Theta} = \mathbf{\Theta}^{(1/2)}\mathbf{\Theta}^{(*/2)}$, and used the property that $|\mathbf{I} - \mathbf{AB}| = |\mathbf{I} - \mathbf{BA}|$ for any matrices $\mathbf{A}$ and $\mathbf{B}$ of compatible dimensions.

Let $\mathbf{V} = \mathbf{\Theta}^{(1/2)}\mathbf{T}\mathbf{\Theta}^{(1/2)}$. Note that since both $\mathbf{T}$ and $\mathbf{\Theta}$ are positive definite, then $\mathbf{V}$ is also positive definite. Moreover,

$$J(\mathbf{T} \to \mathbf{V}) = |\mathbf{\Theta}^{-1}|^{m} = |\mathbf{\Theta}|^{-m}. \tag{62}$$

Substituting (62) into (61) we get

$$\begin{aligned} \text{LHS of (61)} \approx \int_{\mathbf{V}>0} &|\mathbf{\Theta}|^{-m} \cdot |\mathbf{I} - \mathbf{V}| \\ &\cdot |\mathbf{V}\mathbf{\Theta}^{-1}|^{\beta-\alpha-\frac{m}{2}} \cdot |\mathbf{V}\mathbf{\Theta}^{-1} + \mathbf{I}|^{\beta+\alpha-\frac{m}{2}} d\mathbf{V} \\ \approx \int_{\mathbf{V}>0} &|\mathbf{\Theta}|^{-m} \cdot |\mathbf{I} - \mathbf{V}| \\ &\cdot |\mathbf{V}\mathbf{\Theta}^{-1}|^{\beta-\alpha-\frac{m}{2}} \cdot |\mathbf{V}\mathbf{\Theta}^{-1}|^{\beta+\alpha-\frac{m}{2}} d\mathbf{V} \end{aligned} \tag{63}$$

where in (63) we used $|\mathbf{V}\mathbf{\Theta}^{-1} + \mathbf{I}| \approx |\mathbf{V}\mathbf{\Theta}^{-1}|$ since $\|\mathbf{\Theta}\| \to 0$. Rearranging (63) and substituting into (60) gives

$$\begin{aligned} W_{\alpha,\beta}(\mathbf{\Theta}) \approx \frac{|\mathbf{\Theta}|^{\beta+\frac{m}{2}} \cdot e^{-\frac{1}{2}\mathrm{Tr}\mathbf{\Theta}}}{\tilde{\Gamma}_m(\beta - \alpha + m/2)} \cdot |\mathbf{\Theta}|^{-2\beta} \\ \cdot \int_{\mathbf{V}>0.} |\mathbf{I} - \mathbf{V}| \cdot |\mathbf{V}|^{2\beta-m} d\mathbf{V}. \end{aligned} \tag{64}$$

That is

$$\begin{aligned} W_{\alpha,\beta}(\mathbf{\Theta}) \approx e^{-\frac{1}{2}\mathrm{Tr}\mathbf{\Theta}} \cdot |\mathbf{\Theta}|^{\frac{m}{2}-\beta} \\ \cdot \frac{1}{\tilde{\Gamma}_m(\beta - \alpha + m/2)} \int_{\mathbf{V}>\mathbf{0}} |\mathbf{I} - \mathbf{V}| \cdot |\mathbf{V}|^{2\beta-m} d\mathbf{V}. \end{aligned} \tag{65}$$

Note that the integration on the right hand side of (65) yields a constant that is independent of the matrix $\mathbf{\Theta}$, so that we can write (65) as

$$W_{\alpha,\beta}(\mathbf{\Theta}) \approx k e^{-\frac{1}{2}\mathrm{Tr}\mathbf{\Theta}} |\mathbf{\Theta}|^{\frac{m}{2}-\beta} \tag{66}$$

for some constant k.

REFERENCES

[1] S. Shi and M. Schubert, "MMSE transmit optimization for multi-user multi-antenna systems," in *Proc. IEEE Int. Conf. Acoust., Speech, Signal Process.*, Philadelphia, PA, Mar. 2005, vol. 3, pp. 409–412.

[2] K.-K. Wong, R. D. Murch, and K. B. Letaief, "A joint-channel diagonalization for multiuser MIMO antenna systems," *IEEE Trans. Wireless Commun.*, vol. 2, pp. 773–786, July 2003.

[3] Z. Pan, K.-K. Wong, and T.-S. Ng, "Generalized multiuser orthogonal space-division multiplexing," *IEEE Trans. Wireless Commun.*, vol. 3, pp. 1969–1973, Nov. 2004.

[4] A. Bourdoux and N. Khaled, "Joint TX-RX optimization for MIMO-SDMA based on a null-space constraint," in *Proc. IEEE 56th Veh. Technol. Conf.*, Vancouver, Canada, Sep. 2002, pp. 171–174.

[5] Q. H. Spencer, A. L. Swindlehurst, and M. Haardt, "Zero-forcing methods for downlink spatial multiplexing in multi-user MIMO channels," *IEEE Trans. Signal Process.*, vol. 52, pp. 461–471, Feb. 2004.

[6] M. Bengtsson, "A pragmatic approach to multi-user spatial multiplexing," in *Proc. IEEE Sens. Array and Multichannel Signal Process. Workshop*, Rosslyn, VA, Aug. 2002, pp. 130–134.

[7] R. Chen, J. G. Andrews, and R. W. Heath, "Multiuser space-time block coded MIMO system with unitary downlink preceding," in *Proc. IEEE Int. Conf. Commun.*, Paris, France, Jun. 2004, pp. 2689–2693.

[8] R. W. Heath, M. Airy, and A. J. Paulraj, "Multiuser diversity for MIMO wireless systems with linear receivers," in *Proc. 35th Asilomar Conf. Signals, Syst., Comput.*, Philadelphia, PA, Nov. 2001, vol. 2, pp. 1194–1199.

[9] T. Yoo and A. Goldsmith, "Optimality of zero-forcing beamforming with multiuser diversity," in *Proc. IEEE Int. Conf. Commun.*, Seoul, Korea, May 2005, pp. 542–546.

[10] I. Berenguer, X. Wang, and V. Krishnamurthy, "Adaptive MIMO antenna selection via discrete stochastic optimization," *IEEE Trans. Signal Process.*, vol. 53, pp. 4315–4329, Nov. 2005.

[11] D. Gore, R. Heath, and A. Paulraj, "Statistical antenna selection for spatial multiplexing systems," in *Proc. IEEE Int. Conf. Commun. (ICC)*, New York, 2002, pp. 450–454.

[12] R. Heath and A. Paulraj, "Antenna selection for spatial multiplexing systems based on minimum error rate," in *Proc. IEEE Int. Conf. Commun. (ICC)*, Helsinki, Finland, 2001, pp. 2276–2280.

[13] D. Gore and A. Paulraj, "MIMO antenna subset selection with space-time coding," *IEEE Trans. Signal Process.*, vol. 50, pp. 2580–2588, Oct. 2002.

[14] A. Tarighat, M. Sadek, and A. H. Sayed, "A multi user beamforming scheme for downlink MIMO channels based on maximizing signal-to-leakage ratios," in *Proc. IEEE Int. Conf. Acoust., Speech, Signal Process.*, Philadelphia, PA, Mar. 2005, vol. 3, pp. 1129–1132.

[15] M. Sadek, A. Tarighat, and A. H. Sayed, "A leakage-based precoding scheme for downlink multi-user MIMO channels," *IEEE Trans. Wireless Commun.*, 2007, to be published.

[16] K. Wong, R. Cheng, K. B. Letaeif, and R. D. Murch, "Adaptive antennas at the mobile and base stations in an OFDM/TDMA system," *IEEE Trans. Commun.*, vol. 49, pp. 195–206, Jan. 2001.

[17] M. Schubert and H. Boche, "Solution of the multiuser downlink beamforming problem with individual SINR constraints," *IEEE Trans. Veh. Technol.*, vol. 53, no. 1, pp. 18–28, Jan. 2004.

[18] G. Golub and C. V. Loan, *Matrix Computations*, 3rd ed. Baltimore, MD: The Johns Hopkins Univ. Press, 1996.

[19] E. G. Larsson and P. Stoica, *Space-Time Block Coding for Wireless Communications*. Cambridge, U.K.: Cambridge Univ. Press, 2003.

[20] D. K. N. A. K. Gupta, *Matrix Variate Distributions*. New York, : Chapman and Hall/CRC, 2000.

[21] R. J. Muirhead, *Aspects of Multivariate Statistical Theory*. New York: Wiley, 1982.

[22] G. A. F. Seber, *Multivariate Observations*. New York: Wiley, 1984.

[23] A. M. Mathai, *Jacobians of Matrix Transformations and Functions of Matrix Argument*. Singapore: World Scientific, 1997.

[24] A. T. James, "Distributions of matrix variates and latent roots derived from normal samples," *Ann. Math. Stat.*, vol. 35, pp. 475–501, Jun. 1964.

[25] A. G. Constantine, "Some non-central distribution problems in multivariate analysis," *Ann. Math. Stat.*, vol. 34, pp. 1270–1285, Dec. 1963.

[26] A. H. Sayed, *Fundamentals of Adaptive Filtering*. Piscataway, NJ: Wiley-IEEE Press, 2003.

[27] M. Abramowitz and I. Stegun, *Handbook of Mathematical Functions with Formulas, Graphs, and Mathematical Tables*. Washington, DC: U.S. Dept. Commerce, 1972.

[28] A. M. Mathai and G. Pederzoli, "On Whittaker function of matrix argument," *Linear Algebra Its Appl.*, vol. 269, pp. 91–103, 1998.

[29] A. Edelman, "Eigenvalues and condition numbers of random matrices," Ph.D. dissertation, Dept. Math., Mass. Inst. Technol., Cambridge, 1989.

[30] L. Zheng and D. N. C. Tse, "Communication on the Grassmann manifold: A geometric approach to the noncoherent multiple-antenna channel," *IEEE Trans. Inf. Theory*, vol. 48, pp. 359–383, Feb. 2002.

[31] P. Koev and A. Edelman, "The efficient evaluation of the hypergeometric function of a matrix argument," *Ann. Math. Computat.*, vol. 75, pp. 833–846, Jan. 2006.

[32] R. A. Lippert, "A matrix model for the β-Jacobi ensemble," *J. Math. Phys.*, vol. 44, pp. 4807–4816, Oct. 2003.

Mirette Sadek (S'01) received the B.Sc. and the M.Sc. degrees in electrical engineering from Ain Sahms University, Cairo, Egypt, in 1997 and 2001, respectively. She received the M.Sc. and Ph.D. degrees in electrical engineering from the University of California, Los Angeles (UCLA), in 2006.

She is now with Newport Media, Irvine, CA.

Dr. Sadek was the recipient of the Taha Hussein medal of Honor for ranking first in the General Secondary School certificate, Egypt, 1992.

Alireza Tarighat (S'00–M'05) received the B.Sc. degree in electrical engineering from Sharif University of Technology, Tehran, Iran, in 1998. He received the M.Sc. and Ph.D. degrees in electrical engineering from the University of California, Los Angeles (UCLA), in 2001 and 2005, respectively.

During summer 2000, he was with Broadcom, El Segundo, CA, where he worked on designing IEEE 802.11a transceivers. From 2001 to 2002, he was with Innovics Wireless, Los Angeles, working on ASIC implementation of advanced antenna diversity and rake processing for 3G WCDMA mobile terminals. Since 2005, he has been with WiLinx, Los Angeles, developing CMOS solutions for UWB systems. His research interests are in communication systems and signal processing, including MIMO OFDM systems, multiuser MIMO wireless networks, algorithms for impairments compensation, and experimental and practical communication systems.

Dr. Tarighat was the recipient of the Gold Medal of the National Physics Olympiad, Iran, 1993, and the Honorable Mention Diploma of the 25th International Physics Olympiad, Beijing, China, 1994.

Ali H. Sayed (F'01) received the Ph.D. degree in electrical engineering in 1992 from Stanford University, Stanford, CA.

He is Professor and Chairman of electrical engineering at the University of California, Los Angeles (UCLA). He is also the Principal Investigator of the UCLA Adaptive Systems Laboratory (www.ee.ucla.edu/asl). He has more than 270 journal and conference publications, is the author of *Fundamentals of Adaptive Filtering* (New York: Wiley, 2003), is the coauthor of the research monograph *Indefinite Quadratic Estimation and Control* (Philadelphia, PA: SIAM, 1999) and of the graduate-level textbook *Linear Estimation* (Englewood Cliffs, NJ: Prentice-Hall, 2000). He is also coeditor of the volume *Fast Reliable Algorithms for Matrices with Structure* (Philadelphia, PA: SIAM, 1999). He has contributed several articles to engineering and mathematical encyclopedias and handbooks and has served on the program committees of several international meetings. His research interests span several areas, including adaptive and statistical signal processing, filtering and estimation theories, signal processing for communications, interplays between signal processing and control methodologies, system theory, and fast algorithms for large-scale problems.

Dr. Sayed is the recipient of the 1996 IEEE Donald G. Fink Award. He received the Best Paper Award from the IEEE Signal Processing Society in 2002, the Kuwait Prize in Basic Science in 2003, the Frederick E. Terman Award in 2005, a Young Author Best Paper Award in 2005 from the IEEE Signal Processing Society, and two Best Student Paper awards at international meetings. He is also a member of the technical committees on Signal Processing Theory and Methods (SPTM) and on Signal Processing for Communications (SPCOM), both of the IEEE Signal Processing Society. He has served as Editor-in-Chief of the IEEE TRANSACTIONS ON SIGNAL PROCESSING (2003–2005) and is now serving as Editor-in-Chief of the EURASIP *Journal on Applied Signal Processing*. He is serving as General Chairman of ICASSP 2008 and sits on the Board of Governors of the IEEE Signal Processing Society.